Cope Rearrangement and Molecular Reorientation in Solid Bullvalene: A Single Crystal Deuterium NMR Study

S. Schlick,[†] Z. Luz,*[,§] R. Poupko,[§] and H. Zimmermann[‡]

Contribution from The Weizmann Institute of Science, Rehovot 76100, Israel, and the Max-Planck-Institut für Medizinische Forschung, AG Molekülkristalle, D-6900 Heidelberg, FRG. *Received July 29, 1991*

Abstract: Deuterium NMR spectra of single crystals of deuterated bullvalene were recorded in the temperature range −13 °C to +80 °C. The measurements were performed with the magnetic field parallel to the crystallographic *b*-axis where all four molecules in the unit cell are magnetically equivalent. Below about 5 °C the spectrum consists of ten almost symmetrical doublets due to the ten distinct deuterons per bullvalene molecule. Above 5 °C dynamic line broadening effects set in which were quantitatively interpreted in terms of two independent thermally activated processes: (i) symmetric 3-fold jumps about the molecular C_3 axis and (ii) Cope rearrangement combined with molecular reorientation that preserves the crystal symmetry. The kinetic equations for the rates of the 3-fold jumps and the Cope rearrangement processes are respectively, $k_J = 13.6 \times 10^{17} \exp(-19.1/RT)$ and $k_c = 4.02 \times 10^{14} \exp(-15.1/RT)$, where R is in kcal/mol·deg and the k's are in s^{-1}. Deuterium NMR measurements on a powder sample of deuterated bullvalene were also performed and found consistent with those obtained from the single crystals. The results are discussed in comparison with earlier solid state proton and ^{13}C NMR and structural crystallographic measurements.

Introduction

One of the more interesting examples of tautomeric bond shift processes is the Cope rearrangement reaction in bullvalene.[1,2]

Successive bond shift steps of this process permute the ten carbon atoms of the bullvalene molecule between its $10!/3 = 1\,209\,600$ possible isomeric forms. The kinetic parameters of this reaction were extensively studied by various NMR techniques including ^{13}C, ^{1}H, and ^{2}H in isotropic and liquid crystalline solutions.[2-11] The question of whether the Cope rearrangement can also occur in solid bullvalene was a matter of debate for a number of years. Proton NMR measurements[12] of solid bullvalene revealed a sharp drop in the second moment at around 20 °C, indicating the presence of a dynamic process which could be the Cope rearrangement, a whole molecule reorientation, or a combination of both. On the other hand, crystallographic measurements by X-ray and by neutron diffraction techniques[13-15] indicated that bullvalene is highly ordered in the crystalline state. It was therefore concluded that the Cope rearrangement could not take place in crystalline bullvalene implying that the drop in the proton second moment can only be due to symmetric 3-fold jumps about the molecular C_3 axis. It came therefore as a surprise when in 1985 Meier and Earl[16] discovered, using ^{13}C MAS-NMR, that the Cope rearrangement is taking place in solid bullvalene, after all. These authors found that in the temperature range between −60 °C and 85 °C the ^{13}C peaks of the olefinic and aliphatic carbons of bullvalene gradually merge into a single peak, an effect that could only be explained in terms of the Cope rearrangement process. To conform with the high crystal ordering of bullvalene they concluded that "the Cope rearrangement is combined with a rotation of the whole molecule in such a way that the translational symmetry of the crystal is maintained" so that a transformed molecule will orient in the same way in the crystal as it did before the rearrangement process. Their analysis of the results was, however, qualitative, and no exact kinetic parameters for the rearrangement–rotation process were derived. Also, the possibility of an independent process involving whole-molecule jumps remained an open question.

In the present paper we extend the dynamic studies of solid bullvalene using deuterium NMR of single crystals. We confirm the rearrangement–rotation mechanism suggested by Meier and Earl[16] and determine the kinetic parameters for this process between around 0 °C and the melting point of bullvalene (92 °C). We also show that the bullvalene molecules undergo an independent 3-fold jump process, and we determine the rate of this process as well. It thus turns out that solid bullvalene is at the same time a highly order crystalline system and also highly fluxional. It exhibits, both whole-molecule jumps and valence-bond tautomerism but using pathways that leave the site symmetry in the crystal completely unchanged.

The experimental details including the mounting and NMR measurements of the bullvalene single crystals are described in the Experimental Section. The single crystal measurements at low temperatures and in the temperature range where dynamic effects are observed, are then presented and compared with theoretically calculated lineshapes from which kinetic parameters are derived. These parameters are subsequently used to simulate and analyze the spectra obtained from a powder sample of bullvalene. We close with a short summary and conclusions which

[†] On sabbatical leave from the University of Detroit.
[§] The Weizmann Institute of Science.
[‡] Max-Planck-Institut für Medizinische Forschung.

(1) Doering, W. von E.; Roth, W. R. *Tetrahedron* **1963**, *19*, 715.
(2) Oth, J. F. M.; Mullen, K.; Gilles, J.-M.; Schröder, G. *Helv. Chim. Acta* **1974**, *57*, 1415.
(3) (a) Saunders, M. *Tetrahedron Lett.* **1963**, *25*, 1699. (b) In *Magnetic Resonance in Biological Systems*; Pergamon Press: New York, 1967; p 85.
(4) Allerhand, A.; Gutowsky, H. S. *J. Am. Chem. Soc.* **1965**, *87*, 4092.
(5) Gunther, H.; Ulmen, J. *Tetrahedron* **1974**, *30*, 3781.
(6) Nakanishi, H.; Yamamoto, O. *Tetrahedron Lett.* **1974**, *20*, 1803. Additional reference to isotropic solutions of bullvalene may be found in: Mann, B. E. *Prog. NMR Spectrosc.* **1977**, *11*, 95.
(7) Huang, Y.; Macura, S.; Ernst, R. R. *J. Am. Chem. Soc.* **1981**, *103*, 5327.
(8) Yannoni, C. S. *J. Am. Chem. Soc.* **1970**, *92*, 5237.
(9) Poupko, R.; Zimmermann, H.; Luz, Z. *J. Am. Chem. Soc.* **1984**, *106*, 5391.
(10) Poupko, R.; Luz, Z.; Vega, A. J.; Zimmermann, H. *J. Chem. Phys.* **1987**, *86*, 5358.
(11) Boeffel, C.; Luz, Z.; Poupko, R.; Zimmermann, H. *J. Magn. Reson.* **1989**, *85*, 329.
(12) Graham, J. D.; Santee, Jr., E. R. *J. Am. Chem. Soc.* **1966**, *88*, 3453.
(13) Johnson, S. M.; McKechnie, J. S.; Lin, B. T.-S.; Paul, I. C. *J. Am. Chem. Soc.* **1967**, *89*, 7123.
(14) Amit, A.; Huber, R.; Hoppe, W. *Acta Crystallogr.* **1968**, *B24*, 865.
(15) Luger, P.; Buschmann, J.; McMullan, R. K.; Ruble, J. R.; Matias, P.; Jeffrey, G. A. *J. Am. Chem. Soc.* **1986**, *108*, 7825. These authors used the almost orthogonal unit cell $B2_1/c$ instead of the primitive $P2_1/c$ unit cell given in the text. The *b*-axis is, however, common to both classifications. See, also: Luger, P.; Buschmann, J.; Richter, Th.; McMullan, R. K.; Ruble, J. R.; Matias, P.; Geffrey, G. A. *Acta Crystallogr.* **1987**, *A 43*, C-105.
(16) Meier, B. H.; Earl, W. L. *J. Am. Chem. Soc.* **1985**, *107*, 5553.

0002-7863/92/1514-4315$03.00/0

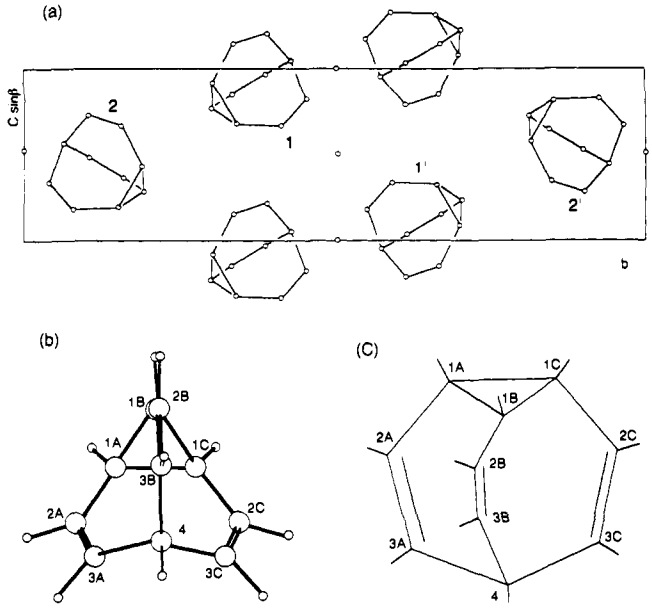

Figure 1. (a) Projection of the crystal structure of bullvalene onto the crystallographic bc^* plane of the monoclinic unit cell. (b) Projection of a single bullvalene molecule down the crystallographic b-axis onto the ac plane. (c) A perspective view of an isolated bullvalene molecule. In the last two diagrams the numbering system used in the present work is given.

also include comparison with the Cope rearrangement in bullvalene solutions and in the related compound semibullvalene.

Experimental Section

Partially deuterated bullvalene (≈50 at %D) was obtained from isotopically normal bullvalene by exchange with *N,N*-dideuterocyclohexylamine/lithium cyclohexylamide as described in ref 10. After the exchange reaction the product was sublimed twice at 10^{-3} Torr. Single crystals were grown from the melt. Under these conditions, bullvalene tends to form twisted crystals. We have therefore carefully screened the crop of crystals under a polarized light stage and for the final measurements selected relatively large specimen (~12 × 4 × 4 mm) which exhibited a minimum degree of twinning.

The deuterium NMR spectra were recorded on a Bruker CXP 300 spectrometer at 46.07 MHz, using the quadrupole echo method. Typical 90° pulse widths were 2.5 μs, and the time interval between $\pi/2$ pulses was 15 μs. The time delay between successive signal accumulations ranged between 300 s at −30 °C to 0.3 s at 85 °C.

The bullvalene crystals usually develop a well-defined crystallographic ac plane. For the single-crystal measurements the specimen was mounted with this plane affixed to the horizontal surface of a semicylindrical perspex stage. The stage with the crystal were snugly fitted into a 5 mm o.d. and 20 mm long NMR tube which was closed at both ends to avoid sublimation of the bullvalene sample during the measurements. The sample tube was fitted into the high power NMR probe with the stage plane roughly oriented perpendicular to the external magnetic field direction. It was then connected to a goniometer that allowed rotation of the sample tube about its long axis. By fine tuning the goniometer screw the crystal was aligned as close as possible with its b-axis parallel to the direction of the magnetic field. This was done by trial-and-error search for the orientation which gave maximum coalescence, i.e., a minimum number of doublets.

For recording of powder spectra the compound was finely crushed, in order to eliminate signals due to coarse graining, before enclosing in a measuring vial.

Results and Discussion

A. The Crystal Structure and the Low Temperature Spectrum of Bullvalene Single Crystals. Bullvalene crystallizes in the monoclinic group $P2_1/c$ with unit cell dimensions (in Å) of a = 6.207, b = 20.785, c = 10.518, and β = 148.34°. There are four molecules per unit cell, but they are arranged in two pairs related by inversion. This is depicted in Figure 1a where a projection of the crystal structure down the a axis onto the bc^* plane is shown; the molecules 1′ and 2′ are obtained by inversion (and translation) of molecules 1 and 2, respectively. Consequently, there are just

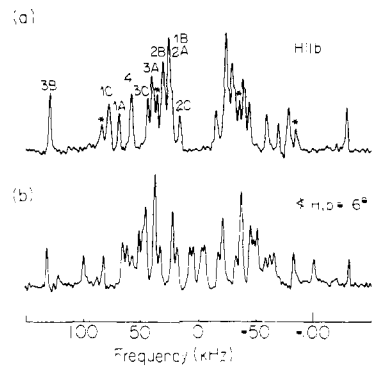

Figure 2. Deuterium NMR spectra at −13 °C of a single crystal of deuterated bullvalene. Trace (a) was taken with the b-axis parallel to the magnetic field, H, while trace (b) was recorded after rotating the crystal by 1.6° about an axis perpendicular to the field direction. In trace (a) the peak assignments in terms of the numbering system of Figure 1b are also given. The asterisks indicate unidentified peaks.

two magnetically inequivalent bullvalene molecules for an arbitrary orientation of the magnetic field. A deuterium NMR spectrum of a single crystal will therefore in general consist of (at most) 20 doublets, corresponding to the 20 magnetically inequivalent deuterons in the two bullvalene molecules. For certain orientations of the magnetic field, however, all four molecules in the unit cell become magnetically equivalent, resulting in a deuterium NMR spectrum of at most ten doublets. These special orientations correspond to the magnetic field lying in the ac plane and along the b axis. To facilitate the analysis of the experimental spectra we chose to measure the single crystals with the magnetic field along one of these special orientations. Since the crystals usually exhibited well developed surfaces parallel to the crystallographic ac planes, it was convenient to mount them, as explained in the Experimental Section, with this plane approximately transverse to the magnetic field and by fine rotation align the b axis as close as possible parallel to the field direction. A spectrum obtained at −13 °C from such an aligned crystal (with peak assignments to be described below) is shown in trace (a) of Figure 2. For comparison we show in trace (b) a spectrum from the same crystal after rotation of 1.6° about an axis perpendicular to the field direction; the degeneracy of the spectrum is lifted, yielding a much more complex pattern. As explained in the Experimental Section we used this sensitivity of the spectrum to the orientation relative to the magnetic field in the final stage of the sample alignment by searching for the orientation which gives a minimum number of peaks.

To identify the peaks in Figure 2a we compare the observed splittings with those expected from the known crystal structure of bullvalene; we assume that the overall quadrupole splitting of each deuterium is given by

$$\nu_Q^i = \frac{3}{2}\left[\frac{e^2qQ}{h}\right]^i \frac{1}{2}[3\cos^2\Theta^i - 1] \qquad (1)$$

where Θ^i is the angle between the magnetic field (the b-axis) and the C–D^i bond direction, and $(e^2qQ/h)^i$ is the quadrupole interaction constant for the particular deuteron. The use of eq 1 assumes that the deuterium quadrupole interaction is uniaxial with the principal tensor component parallel to the C–D bond direction. The exact values of the $(e^2qQ/h)^i$'s differ only slightly from one deuteron to another, and the assignment is, therefore, mainly determined by Θ^i's. In practice we used 272 and 252 kHz for $3e^2qQ/2h$ of respectively the olefinic and aliphatic deuterons in the bullvalene molecule. These values were estimated from the low temperature powder spectrum (see below).

For the determination of the various Θ^i values we use the more recent neutron diffraction data on bullvalene by Luger et al.[15] To facilitate the discussion we show in Figure 1b a projection of one bullvalene molecule onto the ac plane as viewed down the b-axis, i.e., the direction of the magnetic field. The neutron diffraction results show that the C_3 symmetry expected for an isolated

Table I. C–H (C–D) Bond Angles and Deuterium Quadrupole Interaction Constants for a Single Crystal of Bullvalene

C–H/C–D bond no. (i)[a]	angle from b-axis, Θ^{i}[b] (deg)	calcd quad splitting ν_Q^i(calc)[c] (kHz)	obsd quad splitting $\lvert\nu_Q^i\rvert$(exp)[d] (kHz)
1A	147.5	+143	138
1B	115.2	−57	50
1C	150.2	+159	157
2A	115.1	−63	51
2B	65.5	−66	60
2C	118.2	−45	32
3A	68.7	−82	80
3B	9.4	+261	258
3C	71.1	−93	89
4	36.7	+117	118

[a] Numbering system as in Figure 1c. [b] Calculated from crystallographic data of ref 15. [c] Calculated from eq 1 using for the quadrupole interaction parameter, $3e^2qQ/2h$, 252 kHz for the aliphatic deuterons and 272 kHz for the olefinic deuterons. [d] The results correspond to the −13 °C spectrum of Figure 2a. The assignment was made by matching the order and as much as possible the magnitude of the observed splittings with those calculated in the previous column.

bullvalene molecule is very nearly preserved also in the solid. The molecule consists of three almost planar wings which we label A, B, and C, all starting at the bridgehead carbon 4 and ending at the cyclopropane ring carbons 1A, 1B, and 1C (see Figure 1c). The crystallographic b-axis is only 2° away from the plane of the B-wing, while the other two wings (A and C) are nearly symmetrically situated with respect to this axis. In the second and third columns of Table I are shown the angles (Θ^i) between the C–D^i bonds and the crystallographic b-axis as calculated from the data of ref 15 and the expected quadrupole splittings as calculated from eq 1. Comparison with the experimental splittings (fourth column of Table I) immediately provides an assignment for most of the peaks observed in the experiments. Thus, the C–D bond of carbon 3B is almost parallel to the b-axis ($\Theta^{3B} = 9°$) hence it gives the largest splitting in the spectrum (cf. Figure 2a). The C–D bond of the bridgehead carbon 4 is calculated to have $\Theta^4 = 36.7°$ and hence a splitting of ~117 kHz, which is very close to the isolated pair of peaks with $|\nu_Q| = 118$ kHz. Because of the near symmetry of wings A and C, several doublets are expected to appear in clusters of two, i.e., those of deuterons 1A 1C, 2A 2C, and 3A 3C. Such a pair is observed around $|\nu_Q| \sim 150$ kHz and is readily identified with the deuterons 1A and 1C. Similarly, the peaks due to deuterons 3A and 3C are identified with the two doublets having the splittings 80 and 89 kHz, respectively. The other peaks all have calculated Θ^i's (or $180 - \Theta^i$) around 60–65° and hence they are clustered in the narrow range of $|\nu_Q|$ between 40 and 70 kHz. In this region of Θ^i, small errors in the bond angles will cause relatively large errors in the calculated ν_Q^i's, rendering a definite assignment of the experimental peaks much more uncertain. In practice, we have identified the inner doublet ($|\nu_Q| = 32$ kHz) with the 2C deuterons since they gave the smallest calculated splittings and assigned the rest of the peaks (1B, 2A, and 2B) according to the order of their calculated ν_Q^i's. The final assignment, summarized in Table I, also includes the signs of the quadrupole interactions in the various sites. These cannot be determined from the experimental spectrum but are readily obtained from the calculations.

After completing the assignment as discussed above, there were two pairs of peaks left unidentified. They are indicated by asterisks in Figure 2a. We believe that they are due to a small twinned crystal or to slight misalignment causing the magnetic degeneracy of the more sensitive peaks to be lifted. The same effects may also be responsible for the fact that the intensities of the isolated peaks are not identical and for the appearance of shoulders on some of the lines. Partial lifting of the degeneracy will cause selective line broadening and therefore different intensities for different peaks. Spectral distortion may also arise from unresolved dipolar interaction with protons. As the degree of deuteration is only about 50%, most deuterons in the bullvalene molecule have at least one proton as next nearest neighbor. For certain orientation this may yield a dipolar splitting of 2.5–3.0 kHz, thus contributing significantly to the line width and shape of the deuterium peaks.

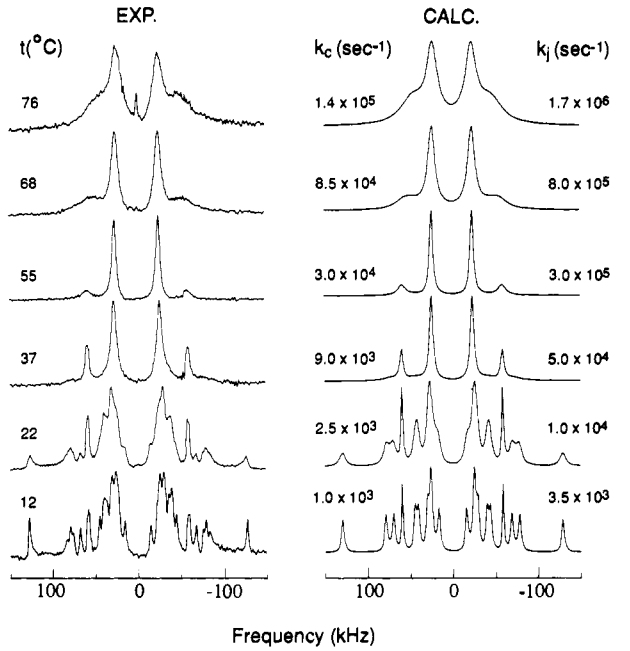

Figure 3. Left: Experimental deuterium NMR spectra from single crystals of deuterated bullvalene aligned with the b-axis parallel to the magnetic field at different temperatures as indicated. Right: Best-fit simulated spectra of the corresponding experimental set. The spectra were calculated using the quadrupole splitting parameters of Table I and the indicated rate parameters k_c and k_j. An exchange independent line width parameter $1/T_2 = 4000$ s^{-1} was included in the computation, except for carbon 4, for which a value of 6000 s^{-1} was used.

B. The Temperature Dependence of the Single Crystal Spectrum. Experimental deuterium NMR spectra of a single crystal also aligned with its b axis parallel to the magnetic field direction are shown in the left column of Figure 3, for different temperatures until close to the melting point. The spectra show line broadening and coalescence effects typical of dynamic processes. Before attempting a quantitative analysis of these spectra we wish to consider the expected dynamic line shapes under the assumption of (i) pure 3-fold jumps and (ii) pure bond rearrangement coupled with reorientation.

In the 3-fold jump process the bullvalene molecules undergo right- or left-hand 120° jumps about the molecular 3-fold symmetry axis. This process will leave deuteron 4 unaffected and will interchange the three groups of nuclei (1A, 1B, 1C), (2A, 2B, 2C), and (3A, 3B, 3C) among themselves. The appropriate kinetic matrix for this process is

$$k_J K_J = k_J \begin{bmatrix} -2 & 1 & 1 & & & & & & & \\ 1 & -2 & 1 & & & & & & & \\ 1 & 1 & -2 & & & & & & & \\ & & & -2 & 1 & 1 & & & & \\ & & & 1 & -2 & 1 & & & & \\ & & & 1 & 1 & -2 & & & & \\ & & & & & & -2 & 1 & 1 & \\ & & & & & & 1 & -2 & 1 & \\ & & & & & & 1 & 1 & -2 & \\ & & & & & & & & & 0 \end{bmatrix} \quad (2)$$

where k_J is the rate constant for the process, and the labels of the rows and columns of the exchange matrix, K_J, are 1A, 1B, 1C, 2A, 2B, 2C, 3A, 3B, 3C, 4. Clearly the peaks due to deuteron 4 are unaffected by this process and therefore remain sharp throughout the dynamic region. The other three groups of doublets undergo line broadening and eventually merge into three doublets yielding a spectrum similar to that observed at low temperatures in liquid crystalline solutions.[9] Simulated spectra for different values of k_J are shown in the left column of Figure 4.

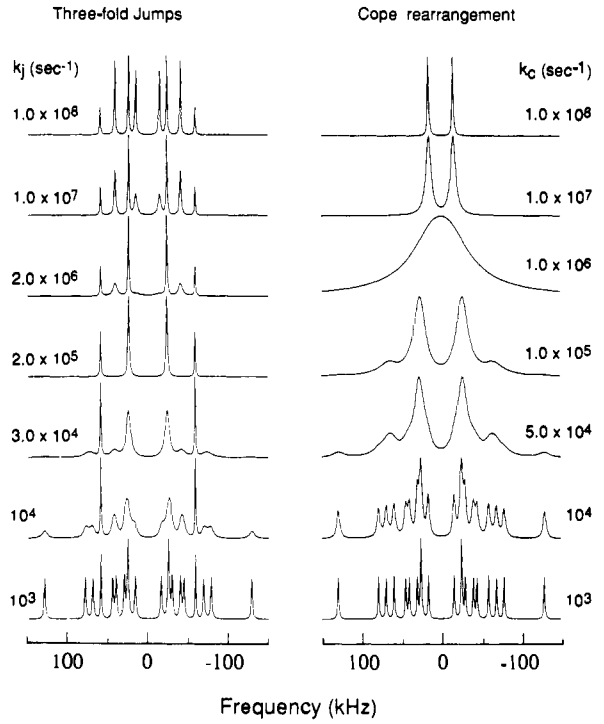

Figure 4. Left: Simulated dynamic spectra for pure 3-fold jumps for the indicated k_j values. Note the invariant peaks due to the deuteron 4 and the merging of all other peaks to three sharp doublets. Right: The same as in the left column but for a pure Cope rearrangement–rotation process. The quadrupole splitting parameters are from Table I, and an exchange invariant line width parameter $1/T_2 = 4000\ s^{-1}$ was assumed.

When discussing the Cope rearrangement–rotation mechanism we must consider two statistical effects. First, we assume that the opening of the cyclopropane ring is equally probable at the three bonds 1A–1B, 1B–1C, and 1C–1A. This assumption neglects crystal-field effects which cause slight distortions of the molecule from perfect C_{3v} symmetry. Depending on which of the three cyclopropane bonds undergoes cleavage, carbon 1C, 1A, or 1B will become the bridgehead atom. In order to preserve the molecular orientation in the crystallographic site the molecule must immediately reorient to bring the new bridgehead atom to the original site of carbon 4 and the newly formed cyclopropane ring (3A, 3B, 4), (3B, 3C, 4), or (3C, 3A, 4), into the original site of carbons 1A, 1B, and 1C. Here too we need to remember that this can occur with equal probability at three different orientations related to each other by 120° rotation about the newly formed C_3 axis. These considerations lead to the following kinetic matrix for the combined Cope rearrangement–rotation mechanism

$$k_c K_c = k_c \frac{1}{9} \begin{bmatrix} -9 & & & & & & 2 & 2 & 2 & 3 \\ & -9 & & & & & 2 & 2 & 2 & 3 \\ & & -9 & & & & 2 & 2 & 2 & 3 \\ & & & -7 & 2 & 2 & 1 & 1 & 1 & \\ & & & 2 & -7 & 2 & 1 & 1 & 1 & \\ & & & 2 & 2 & -7 & 1 & 1 & 1 & \\ 2 & 2 & 2 & 1 & 1 & 1 & -9 & & & \\ 2 & 2 & 2 & 1 & 1 & 1 & & -9 & & \\ 2 & 2 & 2 & 1 & 1 & 1 & & & -9 & \\ 3 & 3 & 3 & & & & & & & -9 \end{bmatrix} \quad (3)$$

where k_c is the rate constant for the reaction and the rows and columns labeling of the corresponding exchange matrix, K_c, is as in eq 2. In this case all deuterons interchange among themselves resulting, in the fast exchange limit, in a single average doublet. The expected evolution of the spectrum under the Cope rearrangement–rotation mechanism as calculated from eq 3 is shown in the right column of Figure 4. Note that in this case all lines undergo broadening and eventually coalesce into a single doublet.

Referring again to the left column of Figure 3 we note that the line shape of the experimental spectra over the whole dynamic range are not reproduced by either the pure 3-fold jump process nor by the pure Cope rearrangement mechanism. Close examination reveals that the characteristic features of the 3-fold jump process appear in the spectrum at low temperatures, while the Cope rearrangement dominates the line shape at high temperatures. These qualitative conclusions follow from the fact that at lower temperatures (<30 °C) all peaks in the spectrum undergo line broadening except the pair assigned to deuteron 4. On the other hand, at higher temperatures the spectrum does not converge into a four doublet pattern as would be the case from pure 3-fold jumps but rather evolves into a single doublet as expected for the Cope rearrangement.

To quantitatively interpret the experimental spectra we therefore assumed that both dynamic processes, the 3-fold jumps and the Cope rearrangement–rotation, occur independently so that the NMR line shape can be described by an overall kinetic matrix of the form

$$K = k_J K_J + k_c K_c \quad (4)$$

With this kinetic matrix dynamic line shapes were calculated and best fitted to the experimental results by varying both k_J and k_c. Since the spectra were recorded by the quadrupole echo method, the time domain signal (second half of the echo) is given by[17]

$$S(t) = Re\ [\mathbf{1} \cdot e^{-R(\tau+t)}\ e^{-R^*\tau} \cdot \mathbf{1}] \quad (5)$$

where τ is the time interval between the $\pi/2$ pulses in the quadrupole echo sequence, $\mathbf{1}$ represents a ten-dimensional vector with all elements equal unity, and the matrix R is

$$R = \pm i\Omega - K + (\mathrm{INT}_2) \quad (6)$$

In this equation INT_2 and Ω are diagonal matrices whose elements are the exchange independent line width parameters and resonance frequencies of the various peaks. The ± signs refer to the $+1 \rightarrow 0$ and $0 \rightarrow -1$ subspectra. In practice, $1/T_2$ was taken as 4000 s^{-1} for all lines except that for carbon 4 a larger value (6000 s^{-1}) had to be used to better fit the experimental results. This probably reflects the fact that Θ^4 is close to 45° where the sensitivity to the orientation of the magnetic field is largest. The resonance frequencies were taken from Table I, and the rate parameters k_J and k_c were varied so as to best fit the experimental spectra. Such best-fit spectra, obtained by Fourier transformation of eq 5, are shown in the right column of Figure 3. As may be seen they reproduce the main features of the experimental results pretty well, in particular the invariance of the doublet due to deuteron 4 at low temperatures and the coalescence of the signals into a single doublet at high temperatures. The fit in the intermediate and high temperature range is quite satisfactory but it is not as good in the very slow exchange regime. We believe that the difficulty arises from small misalignment of the crystal and distortion of the peaks line shape due to dipolar interactions with residual protons in the bullvalene molecule as discussed above.

The results for k_J and k_c obtained by fitting the experimental spectra over the whole temperature range studied are summarized in terms of the two Arrhenius plots in Figure 5. From these plots the following rate equations are derived for the two processes

$$k_J = 13.6 \times 10^{17} \exp(-19.1/RT)$$

$$k_c = 4.02 \times 10^{14} \exp(-15.1/RT)$$

where R is in kcal/mol deg and the k's are in s^{-1}.

C. The NMR Spectrum of a Powder Sample. Additional support for the dynamic model presented in the previous section is obtained from the analysis of the deuterium NMR line shape of a powder sample of deuterated bullvalene. Experimental spectra at different temperatures are shown in the left column of Figure 6. At low temperatures the spectrum is typical of a rigid powder. The perpendicular features of the spectrum exhibit shoulders which we ascribe to the presence of two types of deuterons, i.e., olefinic and aliphatic, with slightly different quadrupole interaction

(17) Vega, A. J.; Luz, Z. *J. Chem. Phys.* **1987**, *86*, 1803.

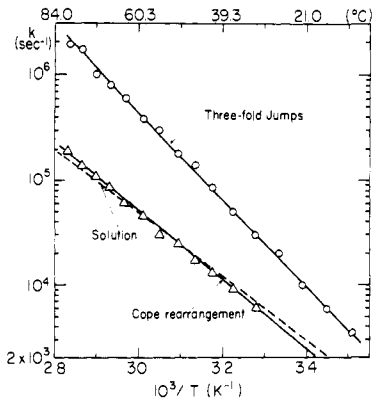

Figure 5. Arrhenius plots for the rate constants of the 3-fold jump process, k_J, and of the Cope rearrangement–rotation reactions, k_c, in solid bullvalene as determined from the temperature dependence of the deuterium NMR line shape of single crystals. The dashed line corresponds to the Cope rearrangement in a liquid crystalline solution.[9]

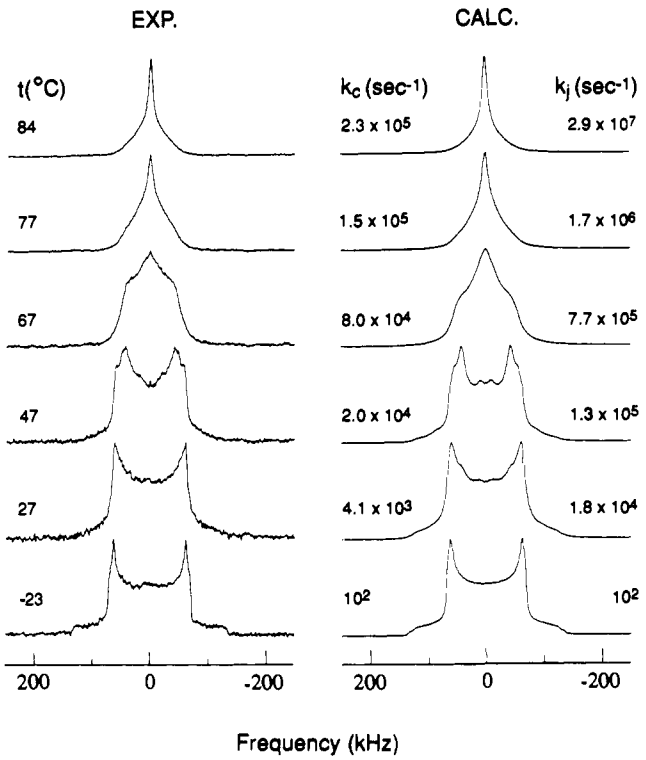

Figure 6. Left: Experimental deuterium NMR spectra of a powder sample of deuterated bullvalene at different temperatures as indicated in the figure. Right: Simulated powder spectra calculated with the indicated rate constants k_J and k_c taken for the corresponding temperatures from Figure 5. An exchange independent line width parameter varying from 13 000 s^{-1} for the −23 °C spectrum to 4000 s^{-1} for the 84 °C spectrum was used.

constants. From the spacings between the shoulders and cusps of the perpendicular features we estimate $3e^2qQ/2h$ values of 272 kHz for the olefinic and 252 kHz for the aliphatic deuterons. As the temperature is increased, line shape changes take place leading at high temperature to a single relatively sharp peak due to the occurrence of dynamic processes. As for the single crystal spectra it is not possible to simulate these spectra in terms of a single dynamic model, i.e., pure 3-fold jumps or the combined Cope rearrangement–reorientation process. Simulated powder spectra for the isolated processes are shown in Figure 7. It may be seen that for the jump model they evolve into a line shape consisting of a superposition of four powder patterns with different axially symmetric quadrupole interactions, while the Cope rearrangement gradually leads to a single powder spectrum with a highly reduced splitting. None of these series of spectra fit the experimental results; however, using the combination of these two processes (eq

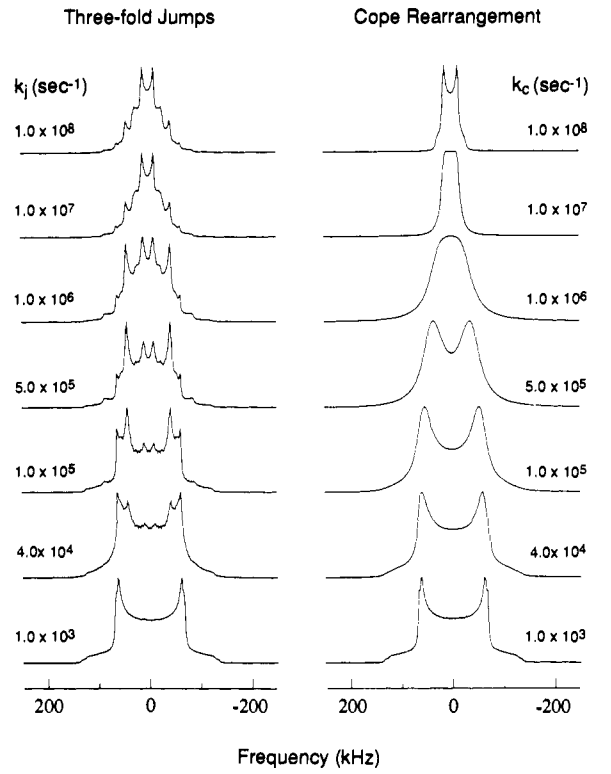

Figure 7. Simulated dynamic deuterium NMR powder spectra of bullvalene under conditions where only 3-fold jumps (left) or only Cope rearrangement with reorientation take place (right). $1/T_2$ was assumed to be 8000 s^{-1}.

4) with the rate constants determined from the single crystal measurements yield satisfactory simulations as shown in the right column of Figure 6. To facilitate the powder line shape calculations we assumed in all cases a perfect C_{3v} symmetry with average bond angles over the three wings of the bullvalene molecule. The fit between the calculated and experimental spectra could probably be improved by using the exact bond angles (rather than averages) and fitting different quadrupole splitting parameters for the various deuterons. We believe, however, that the similarity between the experimental and approximately simulated spectra is sufficient to support the proposed dynamic model.

Summary and Conclusions

Using deuterium NMR of single crystals we have determined the rate parameters of two independent dynamic processes in solid bullvalene. One process consists of symmetric 3-fold jumps of the bullvalene molecules, and the other is a combined process of the Cope rearrangement together with a molecular reorientation which installs the molecules back into their original orientations. Both processes preserve the high molecular order of the crystal deduced from X-ray and neutron diffraction. The results are consistent with all previous studies of ordering and motion in solid bullvalene, in particular with the large drop in the proton NMR second moment observed at around room temperature and with the dynamic spectra observed in the ^{13}C NMR–MAS experiment.

Three-fold jumps of molecules or moieties with C_3 symmetry are often observed in molecular crystals, but they are usually associated with much smaller activation energies. The value of 19.1 kCal/mol determined for bullvalene appears exceptionally high for globular shaped molecules and reflects the very high crystal order as deduced from the crystallographic studies. The activation energy for the Cope rearrangement–rotation process is considerably lower and is almost identical to that observed in liquid solutions (see dashed line in Figure 5). This indicates that the rate of the bond shift process is predominantly governed by the internal potential of the isolated bullvalene molecule. It appears that in the transition state of the bond shift process the molecule becomes "soft", and, unlike in its ground state, it can readily reorient within the crystal. This explains, what might

appear as a contradiction, that below the crossing temperature of the Arrhenius curves (between around -25 and -30 °C) the Cope rearrangement-reorientation process is faster than the pure (3-fold) jump process.

In principle another dynamic process that preserves crystal order should also be considered, i.e., translational self-diffusion. Such a process occurs via molecular diffuse jumps between lattice sites, and for bullvalene we need to consider two situations: (i) When the jumps are between equivalent sites (see Figure 1), they will in general be accompanied by reorientation about the molecular C_3 axes, and the effect on the NMR spectrum will be identical to that for pure 3-fold jumps. (ii) If the diffusive jumps occur between different lattice sites, the process will also involve a change in orientation of the molecular symmetry axes. In the present work we only recorded spectra at magnetic field orientations where all crystal sites were equivalent and therefore only the 3-fold jump part of such diffuse jumps would be felt. We plan to extend our measurements to single crystals at general orientations of the magnetic field in order to determine whether such diffuse jumps occur on the NMR time scale. For now we can only set an upper limit to the self-diffusion constant by assuming that the 3-fold jumps are entirely due to diffusion. Using Einstein's diffusion equation $l^2 = 6Dt$ with l equal to an average lattice distance in bullvalene (~5.6 Å) and t of the order of the correlation time for the 3-fold jumps (~ 10^{-4} s at room temperature) we obtain $D < 5 \times 10^{-12}$ cm^2 s^{-1}. For comparison for adamantane, which has a similar molecular shape, $D \sim 10^{-21}$ cm^2 s^{-1} at room temperature.[18] It is therefore most likely that self-diffusion in bullvalene is too slow to affect the NMR line shape in our measurements, but only additional experiments can tell for sure.

It is interesting to compare our results for solid bullvalene with those of Miller and Yannoni[19] for the analogous process in semibullvalene. In this case the Cope rearrangement in solution is extremely fast[20] and freezes out (on the NMR time scale) only around -170 °C. In contrast, in solid semibullvalene no effect on the ^{13}C MAS-NMR line shape due to the Cope rearrangement was observed up to its melting temperature (-85 °C). Apparently in this case the solid packing energy and the nonglobular shape of the molecule prevents reorientation of the molecules and hence the bond shift from taking place. Yannoni and co-workers have also shown[21] that by annealing semibullvalene the bond isomerization becomes extremely fast, apparently due to introduction of disorder.

Acknowledgment. We thank Professor G. Schröder for a generous gift of a bullvalene sample from which the deuterated compound was prepared. We also thank Drs. T. Bernhard, M. Eisenstein, F. Frolow, and U. Haeberlen for numerous discussions concerning the crystal structure of bullvalene and its deuterium NMR spectrum. One of us (S.S.) thanks the Weizmann Institute of Science for a Rosie and Max Varon visiting professorship and the National Science Foundation for a grant, No. DMR-8718947. This work was supported by the Israel Academy of Sciences, Jerusalem.

Registry No. Bullvalene, 1005-51-2.

(18) Resing, H. A. *Mol. Cryst. Liq. Cryst.* **1969**, *9*, 101.

(19) Miller, R. D.; Yannoni, C. S. *J. Am. Chem. Soc.* **1980**, *102*, 7397.
(20) Cheng, A. K.; Anet, F. A. L.; Mioduski, J.; Meinwald, J. *J. Am. Chem. Soc.* **1974**, *96*, 2887.
(21) Macho, V.; Miller, R. D.; Yannoni, C. S. *J. Am. Chem. Soc.* **1983**, *105*, 3735.

Relationship between Amide Proton Chemical Shifts and Hydrogen Bonding in Amphipathic α-Helical Peptides

Nian E. Zhou, Bing-Yan Zhu, Brian D. Sykes, and Robert S. Hodges*

Contribution from the Department of Biochemistry and the Protein Engineering Network of Centres of Excellence, University of Alberta, Edmonton, Alberta, Canada T6G 2H7.
Received October 7, 1991

Abstract: The relationship between amide proton chemical shift and hydrogen bond length has been investigated for a designed amphipathic α-helical peptide (Ac-Glu-Leu-Glu-Lys-Leu-Leu-Lys-Glu-Leu-Glu-Lys-Leu-Leu-Lys-Glu-Leu-Glu-Lys-NH_2). Four important results were obtained. (1) The secondary chemical shifts ($\Delta\delta_{HN}$) changed periodically in a 3-4 repeat pattern along the peptide chain except for the first three residues at the N-terminal end of the peptide. The amide proton exhibits a large positive chemical shift in the center of the hydrophobic face and a large negative chemical shift in the center of the hydrophilic face. For the amide protons that are hydrogen-bonded between residues in the hydrophobic and hydrophilic faces, their chemical shifts are close to the random-coil values. (2) The $\Delta\delta_{HN}$ values at positions 9 and 13 are correlated with the decrease in the hydrophobicity of the side chain substituted at position 9 (Leu, Ala, and Gly). (3) The amplitude of $\Delta\delta_{HN}$ is dependent upon the amphipathicity of the peptide; that is, a peptide with a higher hydrophobic moment has a greater amplitude of $\Delta\delta_{HN}$. (4) The hydrogen-bond lengths calculated from amide chemical shifts are similar to those measured from computer-modeling experiments of a curved α-helix. These results indicate that the amide proton chemical shift is related to hydrogen-bond length and that a single-stranded amphipathic α-helix in solution is curved and this curved structure causes the upfield shifts of amide protons in the convex side and downfield shifts of amide protons in the concave side.

Introduction

It has long been recognized that ^{1}H-NMR chemical shifts in proteins are sensitive not only to the local electronic structure but also to shielding effects that result from the formation of secondary and tertiary structure upon protein folding.[1] The chemical shifts of amino acids in a protein are generally quite different from random-coil values. This sensitivity of chemical shifts to the secondary structure of proteins has been used to deduce structural information.[2-4] In particular, both theoretical calculations[5,6] and

(1) Wuthrich, K. *NMR of Proteins and Nucleic Acids*; Wiley: New York, 1986.
(2) Pastore, A.; Sandek, V. *J. Magn. Reson.* **1990**, *90*, 165-176.
(3) Szilagyi, L.; Jardetzky, O. *J. Magn. Reson.* **1989**, *83*, 441-449.
(4) Wishart, D. S.; Sykes, B. D.; Richards, F. M. *J. Mol. Biol.* **1991**, *222*, 311-333.

0002-7863/92/1514-4320$03.00/0